Excitation-Wavelength Dependence of Fluorescence Intermittency in CdSe Nanorods

Kenneth L. Knappenberger, Jr.,[†] Daryl B. Wong,[†] Wei Xu,[†] Adam M. Schwartzberg,[†] Abraham Wolcott,[‡] Jin Z. Zhang,[‡] and Stephen R. Leone[†,*]

[†]Departments of Chemistry and Physics, University of California and Lawrence Berkeley National Laboratory, Berkeley, California 94720, and [‡]Departments of Chemistry and Biochemistry, University of California, Santa Cruz, California 95064

ABSTRACT The influence of excitation wavelength and embedding media on fluorescence blinking statistics of 4 nm × 20 nm cadmium selenide (CdSe) nanorods is investigated. Photon antibunching (PAB) experiments confirm nonclassical emission from single CdSe nanorods that exhibit a radiative lifetime of 26 ± 13 ns. The blinking data show behaviors that can be categorized into two classes: excitation near the energy of the band gap and at energies exceeding 240 meV above the band gap. Excitation at the band gap energy ($\lambda \geq 560$ nm) results in more pronounced "on" time probabilities in the distribution of "on" and "off" events, while those resulting from excitation exceeding the band gap by 240 meV or more ($\lambda \leq 560$ nm) are 200 times less likely to display continuous "on" fluorescence persisting beyond 4 s. The "off" time statistics are also sensitive to the excitation wavelength, showing a similar, but inversely correlated, effect. To understand better the excitation-wavelength dependence, fluorescence measurements are obtained for single nanorods deposited both on a bare microscope coverslip and embedded in 1-ethyl-3-methylimidizolium bis(trifluoromethylsulfonyl)imide room-temperature ionic liquid (RTIL). The embedding RTIL medium has a significant influence on the resultant fluorescence statistics only when the excitation energy exceeds the 240 meV threshold. The results are explained by a threshold to access nonemissive trap states, attributed to self-trapping of hot charge carriers at the higher photon excitation energies.

KEYWORDS: fluorescence intermittency · CdSe nanorod · photon antibunching · trap-state quenching · single molecule · ionic liquids

Semiconductor nanocrystals and nanorods represent a promising class of inorganic materials with size- and shape-tunable properties. In particular, the facile laboratory synthesis[1] of CdSe nanoparticles with ever-increasing monodispersity has stimulated expectations for devices with optical properties that are continuously tunable across the visible spectrum, including quantum dot lasers,[2] hybrid photovoltaics,[3] and biological labels.[4] Recently, synthetic protocols have been extended to enable formation of 1-D nanorods.[5] The elongated dimension of the nanorod is suggested to provide better charge mobility than 0-D nanocrystals and, hence, enhanced performance in photovoltaic devices.[6] Unfortunately, nanoparticle "trap" states often result in losses that may be detrimental to performance of nanoparticle-based devices. These trap-state losses are reflected in decreased photoluminescence quantum yields, and at the single-particle level, nanocrystals and nanorods display fluorescence intermittency or "blinking", exhibiting power-law statistics over many decades in time.[7−15] These random interruptions of nanoparticle fluorescence emission, likely due to charge carrier trapping, can diminish the efficiency of devices based on single nanocrystals. Understanding the blinking mechanism is a necessary step for the ultimate implementation of nanocrystal- and nanorod-based devices.

Although fluorescence intermittency in semiconductor nanoparticles has been an area of intense research, a unifying physical picture that accounts for the large dynamic range in both time and probability associated with fluorescence blinking has not fully emerged. Power-law-distributed blinking statistics extending over more than eight decades of probability and six decades in time have been reported,[8−15] and such statistics are now accepted as a hallmark of nanoparticle blinking. Two models have been developed to account for these power-law distributions: diffusion of trap-state energies involved in the cycling between emissive and nonemissive configurations[16−19] (called diffusion-controlled charge transfer) and a charge carrier trapping model based on Auger-assisted ionization.[10,20] Diffusion-controlled charge transfer models account for power-law statistics in CdSe nanocrystals by invoking slow diffusion of the energies of bright and dark states. In this model, a nanoparticle blinks from "on" to "off" when the energy of a nonemissive state becomes resonant with the emissive one, traps the charge

*Address correspondence to srl@berkeley.edu.

Received for review July 3, 2008 and accepted August 26, 2008.

Published online September 13, 2008.
10.1021/nn800421g CCC: $40.75

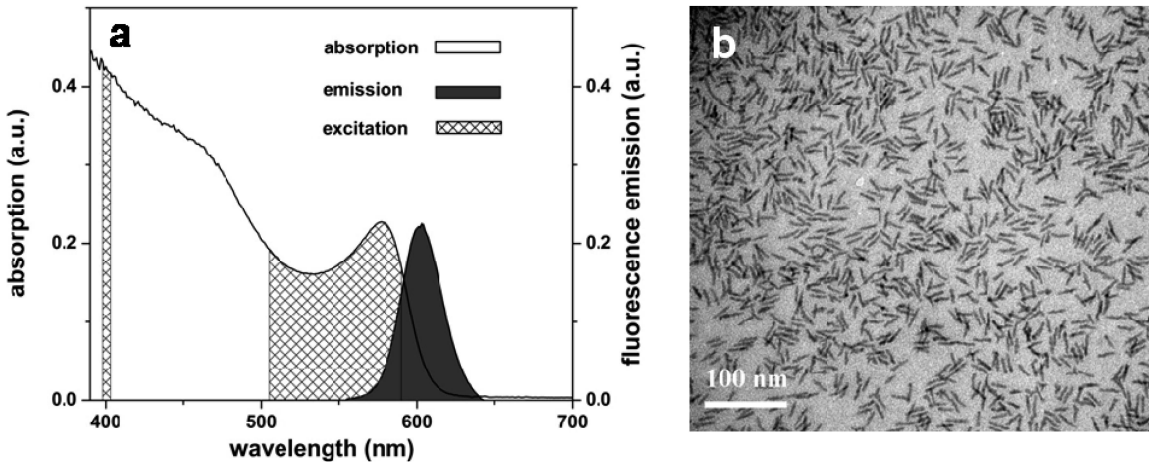

Figure 1. (a) Bulk linear absorption and photoluminescence (PL) spectra of 4 nm × 20 nm CdSe/TDPA nanorods. The global PL (black fill) is obtained from excitation with the 515 nm line of an Ar^+ laser. All measurements are performed at room temperature. The excitation wavelengths used in this work (400 and 510−575 nm) are filled with cross-hatched lines. (b) Transmission electron microscopy (TEM) image of CdSe nanorods dispersed in toluene. The average size of the nanorods is on the order of 4 nm × 20 nm.

carrier, and diffuses in energy. The particle will remain in the "off" state until the energy of the dark state diffuses to match that of the bright state, satisfying the resonance condition for back charge transfer. Diffusion of the trap-state energies is believed to be photodriven, and the effect is related to the observed spectral diffusion of nanocrystal fluorescence.[21,22] The Auger-assisted ionization (trapping) model, which includes a trapping-recovery tunneling mechanism, emerged from the original report of Nirmal *et al.*[7] that attributed CdSe quantum dot blinking to an Auger-assisted ionization process, based on the premise that a quantum dot with a net charge is nonemissive. Evidence for charge formation upon "photodarkening" was subsequently reported.[23] However, this model predicts a single-exponential recovery rate for the emission, whereas power-law statistics are observed. This discrepancy can be reconciled by considering a distribution of trap states with different recovery rates. While these models have been developed to account for existing data on 0-D quantum dots, much less is known about the nature of blinking in elongated 1-D nanorods. Power-law statistics have also been reported for nanorods.[13,14,24,25] However, it is not known whether excitation by one photon will result in uniform fluorescence over the length of the rod or if domains will form, resulting in multiple absorption and emission sites on a single nanorod.

Here we report on the excitation wavelength-dependent blinking statistics of 4 nm × 20 nm CdSe nanorods that are passivated with tetradecylphosphonic acid (TDPA). The uniform emission behavior from single nanorods is corroborated by photon antibunching experiments. For blinking studies, the particles are excited at several wavelengths at and above the band gap (Figure 1a), up to approximately 1.3 eV above the peak of the photoluminescence emission. This extends our previous work[15] on 4 nm CdSe/ZnS core/shell quantum dots by including several more excitation wavelengths across the visible region and also by investigating the importance of particle shape on fluorescence intermittency. This is the first investigation on the influence of excitation wavelength on nanorod blinking. The wavelength-dependent results reported here exhibit two types of blinking behavior: one that occurs when the sample is excited at or near the optical band gap and the other occurring when the excitation is well in excess of the band gap. The transition between these two types of behaviors is step-like with excitation energy, suggestive of an energetic threshold. The creation of the electron−hole pair with an energy 240 meV in excess of the optical band gap results in less pronounced long-duration continuous "on" emission events and results in longer "off" periods. The influence of an external dielectric fluid on the blinking is also shown to depend on the excitation wavelength. Blinking statistics obtained from nanorods embedded in 1-ethyl-3-methylimidizolium bis(trifluoromethylsulfonyl)imide room-temperature ionic liquid (RTIL) show frequent quenching events when the sample is excited above an energetic threshold of approximately 240 meV. However, the RTILs have no influence on the blinking statistics when the excitation energy is below the threshold. This provides evidence for an excitation wavelength-dependent self-trapping mechanism that contributes to nanoparticle blinking. These results establish fluorescence intermittency statistics as a viable tool to better understand charge transfer processes occurring at nanoparticle interfaces.

RESULTS AND DISCUSSION

The bulk room-temperature linear absorption and global photoluminescence (PL) spectra of the CdSe/TDPA nanorods are shown in Figure 1a. The PL spec-

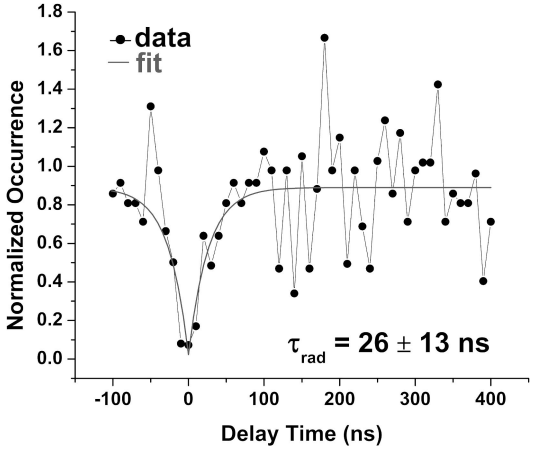

Figure 2. Typical photon-pair histogram obtained for single CdSe/TDPA nanorods. The dip in the occurrence of photon pairs at zero time delay is a hallmark of emission from a single fluorophore. The solid line corresponds to an exponential fit of the histogram. The exponential lifetime (26 ± 13 ns) reflects the radiative lifetime of the nanorods.

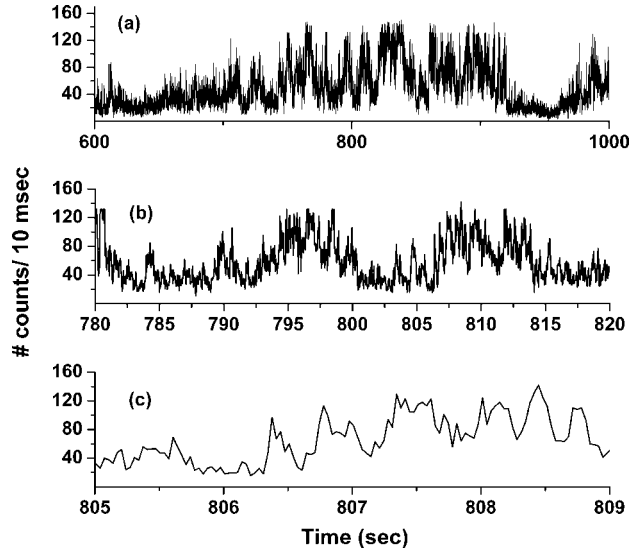

Figure 3. Fluorescence trajectory obtained from a single CdSe/TDPA nanorod. The fluorescence trajectory is recorded by continuously measuring the 605 nm band edge emission. The same fluorescence trajectory is plotted on three different timescales in panels a, b, and c. The random interruption of nanoparticle fluorescence occurs on all measureable timescales, as is the case with CdSe nanocrystals.

trum is plotted normalized to the sample absorption (the $1S_e-1S_h$ transition at 575 nm) for comparison. The peak of the first exciton absorption transition is centered at 575 nm, and the absorption increases continuously to more energetic wavelengths. The peak of the PL is Stokes-shifted from the absorption by approximately 30 nm to a center value of 605 nm, and it has a full-width at half-maximum of 35 nm. From the bulk absorption and PL measurements, a CdSe diameter of approximately 4.0 nm can be inferred.[26] A representative transmission electron microscope (TEM) image of the resultant *ca.* 4 nm × 20 nm CdSe nanorods is shown in Figure 1b.

First, the nature of fluorescence emission of single CdSe nanorods is studied by photon antibunching (PAB).[27,28] The PAB experiments are conducted using 470 nm excitation while recording the 605 nm band edge fluorescence emission. A typical photon-pair histogram representative of more than 50 nanorods studied is shown in Figure 2. The clear dip in the correlation at zero time delay indicates the measured fluorescence is from a single particle with a single emission site. The number of fluorescence emission sites present in the interaction region can be determined by fitting the photon-pair histogram with eq 1.[28−33]

$$g^2(t) = 1 - \frac{1}{N}e^{-t/\tau_{rad}} \qquad (1)$$

Here N is the number of fluorescence emitters or emission sites within the confocal excitation volume, and τ_{rad} is the radiative lifetime of the particle. The fit value for N is 1.1, consistent with previously reported values from single fluorescent molecules[34] and quantum dots.[35] The radiative lifetime is 26 ± 13 ns, and this value is in good agreement with previous reports of tens of nanosecond lifetimes for CdSe quantum dots.[36−38] Taken together, the spectrally and time-resolved absorption and fluorescence measurements noted above and reported in Figures 1 and 2 indicate the optical properties of 4 nm × 20 nm 1-D nanorods are very similar to 0-D quantum dots of a few nanometer size. Importantly, these results confirm not only that the fluorescence measurements are from single nanorods but also that in this size range (4 nm × 20 nm) multiple absorption and emission sites do not exist in these small single particles. As a result, the fluorescence blinking statistics reported below from single nanorods can be compared directly with previous work on single CdSe quantum dots.

Fluorescence trajectories are obtained for single CdSe/TDPA nanorods. A typical fluorescence trajectory resulting from excitation at 400 nm with an average excitation power density of 100 W/cm^2 and 10 ms integration is shown in Figure 3. For each excitation wavelength, a range of power densities spanning 50 W/cm^2 to 15 kW/cm^2 is employed. Although the laser is pulsed at 200 kHz, we see no indication of power density effects. The blinking phenomenon of single quantum dots is evidenced by multiple interruptions of the particle's fluorescence emission at random intervals. Fluorescence trajectories are shown over three different time scales in Figure 3a−c, which exemplify the random nature of the fluorescence blinking in CdSe nanorods, spanning a large time range. This behavior is similar to that of single nanocrystals.[8,15] The blinking statistics are analyzed by creating a probability distribution of "on" and "off" events of a given duration by first converting the fluorescence trajectory into a binary data set. The data are sorted into "on" and "off" categories by assign-

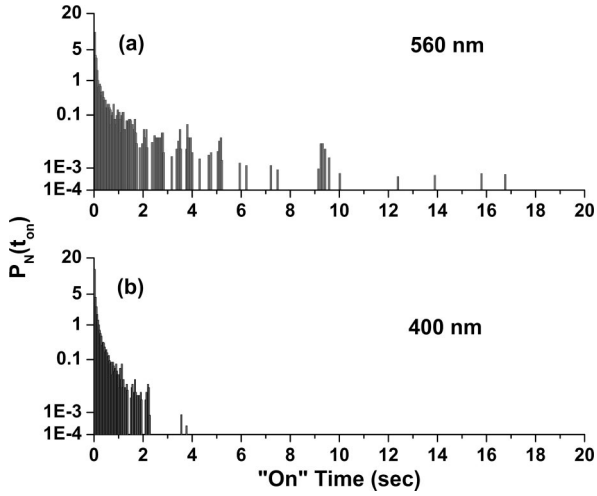

Figure 4. Wavelength-dependent "on"-time probability distribution for CdSe/TOPO nanorods excited with 560 nm (a) and 400 nm (b). The probabilities are plotted on a logarithmic scale as the dependent term. The "on"-time is plotted as the independent term on a linear scale. These plots highlight the wavelength-dependent effect, showing the decreased probability of continuous fluorescence emission beyond a few seconds when the nanoparticle is excited with the more energetic wavelength.

ing a threshold, above which the quantum dot is considered "on" and below which it is considered "off". The threshold level is assigned as twice the standard deviation above the average background counts. This procedure is similar to that used previously.[8,15] For the analysis of "on" and "off" probabilities, it is sufficient to sort the data in this binary manner. However, as is the case for nanocrystals, a histogram of the fluorescence count levels shows a distribution of signal levels for the "on" states, and the data clearly do not correspond to a single "on" intensity value, or even a single Gaussian or Poisson distribution of these levels.[15,20,38] The complexity of the histogram suggests that a distribution of both emissive and nonemissive states is most likely responsible for the blinking mechanism, as suggested for nanocrystals.

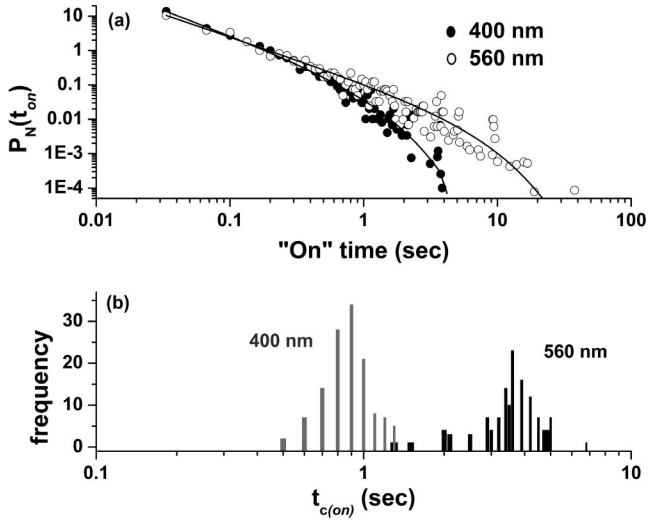

Figure 5. (a) Wavelength-dependent normalized "on" probabilities for individual CdSe/TDPA nanorods excited at 560 nm (○) and 400 nm (●), plotted on a log−log scale. The "on" statistics exhibit strong wavelength dependence. The solid lines represent fits of the data to eq 2. The histograms of $t_{c(on)}$ values for excitation at both 560 nm (black) and 400 nm (gray) are compared in panel b. The histograms include the values of $t_{c(on)}$ obtained from 130 individual nanorods. The comparison clearly shows two different fit results that depend on the excitation wavelength. The fitting results for all 10 excitation wavelengths used are reported in Table 1.

The distribution of "on" probabilities displays significant sensitivity to the excitation wavelength, as shown in Figure 4. The "on" probabilities arising from excitation with 560 and 400 nm light are displayed on semilogarithmic plots in panels a and b of Figure 4, respectively. Here the probabilities are plotted on a logarithmic scale as the dependent variable, and time is the independent variable plotted on a linear scale. This plot clearly illustrates the propensity for longer "on" events when the nanorods are excited at the band gap with 560 nm. Long fluorescence events, beyond a few seconds, are not observed when the more energetic excitation wavelength (400 nm) is used. The probability distributions for both "on" and "off" events are fit to the quantitative model shown in eq 2.

$$P(t_{on/off}) = A t_{(on/off)}^{-\alpha_{(on/off)}} e^{-t_{(on/off)}/t_{c(on/off)}} \quad (2)$$

This model represents a truncated power law, which corresponds to events that are power-law distributed at short times, but exponential for long times. The term $t_{c(on/off)}$ is a fit parameter that corresponds to the critical time at which the probability distribution for continuous "on" or "off" times, $P(t_{on/off})$, switches from a power law with an exponent of $-\alpha_{on/off}$ to an exponential form. Equation 2 has been used previously to fit nanoparticle blinking statistics.[14,15,39] The raw "on" data and fitting results are plotted in Figure 5a for 560 and 400 nm excitation. Attempts were made to fit the data to both an exponential and stretched exponential distribution; however, the best χ^2 value was achieved using eq 2. The short duration events that persist for less than 1 s are power-law distributed for both excitation wavelengths; however, the lower probability long-time events deviate from the power-law distribution at a critical time $t_{c(on)}$. The fitting results from the 10 excitation wavelengths used are reported in Table 1. Histograms of the $t_{c(on)}$ values from both 400 and 560 nm excitation wavelengths obtained from fits to 130 nanorods are compared in Figure 5b. The power law exponent, $-\alpha_{on}$, is not sensitive to the excitation wavelength. However, the critical time ($t_{c(on)}$), the point at which the probability distributions begin to deviate from power-law statistics, is wavelength-dependent. The histogram of fit results (Figure 5b) represents the spread of $t_{c(on)}$ values that results from sample heterogeneity, typical of colloidal nanoparticles, but also shows that the excitation-wavelength dependence is clearly distinguishable. The $t_{c(on)}$ values reported in Table 1 can be classified into two categories: (1) excita-

TABLE 1. Summary of Fitting Results for "On" and "Off" Probabilities[a]

excitation wavelength	α_{on}	$t_{c(on)}$	α_{off}	$t_{c(off)}$
400	1.4 ± 0.2	0.8 ± 0.3	1.2 ± 0.3	2.3 ± 0.3
510	1.4 ± 0.1	0.9 ± 0.3	1.3 ± 0.2	2.1 ± 0.3
520	1.5 ± 0.2	0.9 ± 0.3	1.3 ± 0.2	1.7 ± 0.2
530	1.3 ± 0.1	1.0 ± 0.4	1.2 ± 0.3	1.4 ± 0.3
543	1.3 ± 0.2	1.2 ± 0.4	1.2 ± 0.2	1.5 ± 0.2
550	1.3 ± 0.2	2.7 ± 0.8	1.2 ± 0.2	0.9 ± 0.3
560	1.3 ± 0.1	3.6 ± 0.7	1.4 ± 0.3	0.6 ± 0.2
565	1.2 ± 0.2	3.5 ± 0.5	1.4 ± 0.2	0.6 ± 0.3
570	1.2 ± 0.2	3.9 ± 0.7	1.4 ± 0.2	0.5 ± 0.2
575	1.3 ± 0.2	3.7 ± 0.7	1.5 ± 0.3	0.6 ±0.2

[a]Values reported are obtained from the average and standard deviation of approximately 130 samples at each excitation wavelength. Standard deviations are reported to ±2σ. The dashed line represents the experimentally observed excitation threshold that results in reduction of continuous nanorod fluorescence.

tion near the optical band gap resonance and (2) those resulting from excitation above an approximate 240 meV energetic threshold. This effect is shown clearly by the summary plot in Figure 6, which reports the average critical time for the "on" data ($t_{c(on)}$) along with the standard deviation for 130 individual nanorods. A complementary effect is also observed in the "off" statistics, reported in Table 1.

The change to early truncation times in the "on" probability distribution occurs with 543 nm excitation, and all the "on" distributions from excitation wavelengths shorter than 543 nm show similar results, summarized in Figure 6 and Table 1. The step-like transition in the value of the fitting parameter, $t_{c(on)}$, is clearly shown in Figure 6 and is denoted by the dashed line in Table 1. The "on" statistics obtained when the nanorod is excited near the band gap resonance (560 nm), Figure 5, exhibit a good fit to a truncated power-law normalized probability distribution with a slope α_{on} of 1.3 ± 0.1, and the critical time occurs at 3.6 ± 0.7 s. Furthermore, "on" events persisting for times approaching 100 s are observed. Likewise, excitation in the range spanning 550 to 575 nm produces similar probability distributions. However, when exciting with wavelengths shorter than or equal to 543 nm, there is a curvature in the probability distribution plot due to much less pronounced "on" events of long duration that occurs at earlier times. The example shown in Figure 5, using 400 nm light, results in a $t_{c(on)}$ time of 0.8 ± 0.3 s. The probability of observing continuous fluorescence persisting for 4 s decreases by a factor of 200 when the more energetic excitation is used, as compared to when excitation is near the band gap resonance. This effect is more dramatic for nanorods than observed in CdSe quantum dots,[15] where a reduction of this magnitude occurs only after 10 s.

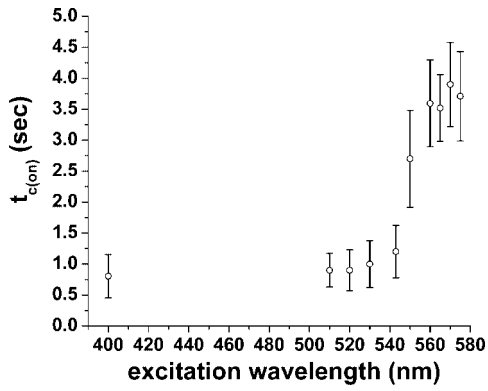

Figure 6. Summary of fit results. The average and standard deviation (2σ) from 130 CdSe nanorods are reported for the value $t_{c(on)}$ in eq 2. The values are obtained with 10 excitation wavelengths, and the results clearly fall into two distinct categories: excitation at the band gap and excitation in excess of the band gap.

The power-law distributions for both the "on" and "off" statistics reported here for CdSe/TDPA nanorods are similar to those observed previously for nanocrystals.[8−15,20] In general, however, the propensity for long continuous "on" emission is decreased for nanorods, as compared to nanocrystals. This effect may result from an increase in the overall number of trapping sites that the charge carriers can encounter in the nanorod. The dependence of the blinking statistics on the excitation wavelength is very similar to that for nanocrystals, albeit with earlier truncation times.[15] The truncation of the "on" probabilities results from a decrease in the number of long continuous "on" times. The observation that excitation above a certain energy results in less continuous fluorescence may be due to an energetic threshold for a charge carrier to access spatially distant trapping sites either on the surface or external to the nanorod. The reported electron escape depth for CdSe quantum dots is 1.5 nm.[40] This value is similar to, although slightly less than, the radius of the nanorods considered here. As a result, a small barrier for a charge to access the surface is expected. The 240 meV threshold reported here from the blinking data likely reflects this barrier. With more energetic excitation wavelengths, charges can more readily escape to the nanoparticle surface, and these hot carriers can access the more distant trap states, possibly in the nanoparticle's surroundings. Further, the nanoparticle surface and surroundings are heterogeneous[41] and may

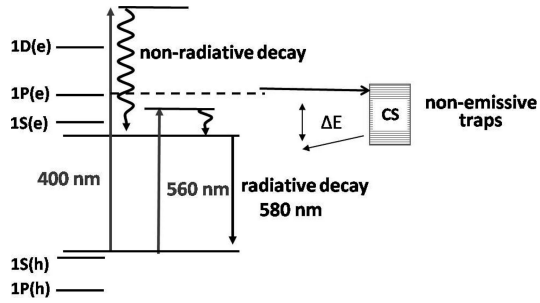

Figure 7. Energy level diagram showing the $1S_e$, $1P_e$, and $1D_e$ delocalized valence band states, as well as the $1S_h$ and $1P_h$ delocalized conduction band states. The vertical upward pointing arrows correspond to excitation of an electron from the conduction band to the valence band. The wavy downward pointing arrows represent ultrafast electronic relaxation of the electron to the bottom of the conduction band. The resultant electron−hole pair that forms can recombine radiatively, by emitting a fluorescent photon, depicted by downward pointing arrow. Alternatively, one of the charges may become localized in a trap state. A possible configuration is the charge-separated (CS) state, where one of the charges is transferred to an external trapping site. The data suggest an energetic threshold (dashed line) must be surmounted to access these external traps.

result in a deeper trapping of the charge. The decrease in long "on" periods, and the corresponding increase in long "off" periods, following excitation above an energetic barrier (240 meV) suggests a transient charge-separated state is formed, which nonradiatively recombines over longer times (*i.e.*, self-trapped exciton).[42] It is worth noting that photoluminescence excitation (PLE) experiments on CdSe quantum dots reveal a dramatic 50% reduction of fluorescence quantum yield when the excitation energy is tuned from the band gap resonance to an energy that exceeds it by 300 meV.[43] This reduction is attributed to an unidentifiable nonradiative recombination process that is very competitive with radiative decay.

A model is depicted schematically in Figure 7. Upon vertical excitation, the electron relaxes nonradiatively to the bottom of the conduction band, within a few hundred femtoseconds, as it dissipates excess energy to discrete phonon modes.[44−46] Subsequently, radiative recombination of the electron−hole pair may occur over a period of several nanoseconds, or the electron may fill the few hundred millielectronvolt trap-state bath *via* phonon-assisted mechanisms.[47] In fact, fluorescence quenching *via* charge filling of trap states has been observed for bulk samples.[48] Trap-state filling has been observed over tens of picoseconds,[49] while a fluorescence lifetime of 26 ± 13 ns is measured for this sample, using the time-correlated single-photon counting technique. The comparatively long radiative lifetime provides ample opportunity for charges to access traps. When enough energy is available in the excitation, a hot carrier is created. This excited charge carrier may be able to sample external traps, creating a charge-separated species that remains in a nonemissive state for long periods, resulting in an overall reduction of the "on" times and increased long "off" times.

The wavelength dependence of the power-law statistics is consistent with an external charge-trapping model. Power-law statistics represent an exponentially large number of observed time bins for continuous fluorescence emission, with a frequency of occurrence that decreases exponentially with increasing time. This can be correlated to a large number of internal and external trap states in proximity to the nanorod that have an exponentially decreasing probability of being populated with increasing distance from the core. Previous NMR experiments provide evidence for the existence of multiple different internal and external structures for both the cadmium and selenium atoms.[41] This disorder may result in formation of trap sites at the surface that differ from those formed in the internal region of the particle. The increasing kinetic energy of a charge carrier, with increasing excitation energy, enables the sampling of more distant trap states, but these trap states have a significantly lower probability of being populated than those close to the core. As a result, it is the long-time low-probability events that are sensitive to the excitation wavelength. On the other hand, the short time, higher probability events are not influenced by the excitation wavelength, as shown by the insensitivity of the slope, α_{on}, reported in Table 1.

To investigate the possibility that the wavelength dependence results from a barrier to create a self-trapped exciton, single nanorod fluorescence is measured in a solvent with known high dielectric constant and conductivity. Stabilization of a charge-separated state should be highly dependent on the surrounding dielectric environment. The stabilization energy of a charge-separated state is directly proportional to the dielectric constant of the surrounding cavity.[50] Trajectories from CdSe/TDPA nanorods embedded in 1-ethyl-3-methylimidizolium bis(trifluoromethylsulfonyl)imide room-temperature ionic liquid (RTIL) with a dielectric constant of 12.3[51] are measured with excitation energies of 30 and 240 meV above the optical band gap. The latter case is just above the energetic threshold observed for the transition in the blinking statistics. The "on" time probabilities of drop-coated nanorods and nanorods in the RTIL are plotted for the 30 meV data on a log−log scale in Figure 8. The solvent shows no influence on the statistics over the six decades in probability or five decades in time over which the probabilities are plotted. This finding indicates that when nanorods are excited near the band gap resonance, the environment has little or no influence over the fluorescence statistics.

Fluorescence trajectories of single CdSe/TDPA nanorods excited 240 meV above band gap are shown in Figure 9, for drop-coated samples (panel a) and samples embedded in RTILs (panel b). In addition to a decrease in the number of "on" events, there is a reduction in the

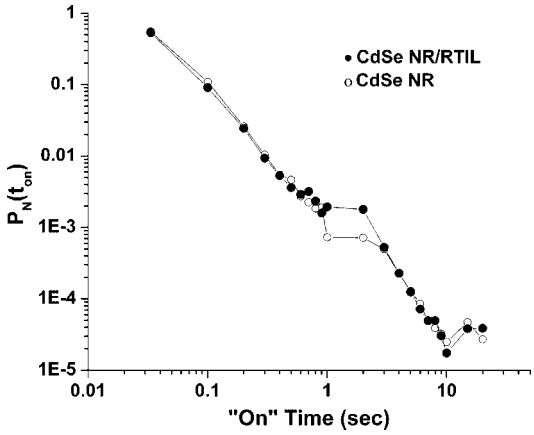

Figure 8. Normalized "on"-time statistics resulting for CdSe/TDPA nanorods drop cast to clean microscope coverslips (○) and when embedded in 1-ethyl-3-methylimidizolium bis(trifluoromethylsulfonyl)imide room-temperature ionic liquids (RTILs) (●). The excitation energy is 30 meV above band gap, and the power density is 80 W/cm^2. The RTILs show no influence on the blinking statistics at this excitation wavelength.

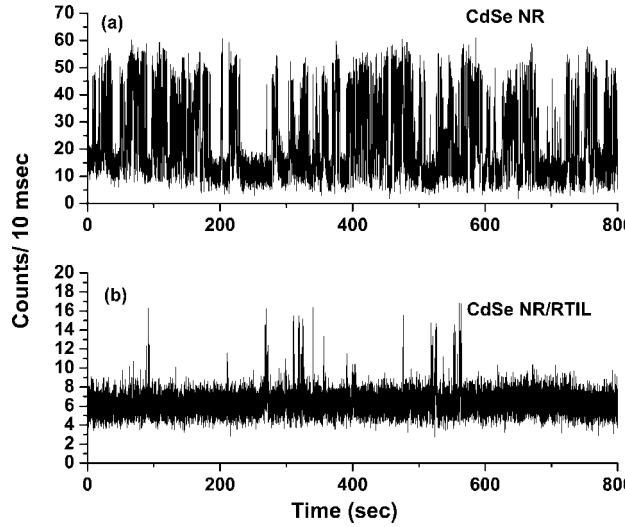

Figure 9. (a) CdSe/TDPA nanorod fluorescence trajectory obtained from 543 nm (240 meV above band gap) excitation and power density of 80 W/cm^2. The excitation is 240 meV in excess of the experimentally observed energetic barrier. (b) CdSe/TDPA fluorescence trajectory from nanorod embedded in RTIL. A clear decrease in the frequency of "on" events, as well as a reduction of the overall fluorescence photon count rate is observed.

overall photon count rate in panel b. The "off" statistics plotted in Figure 10 show the effect of the RTIL clearly, as there is a dramatic increase in the probability of long off events. The slope, α_{off}, for the "off" statistics of drop-coated nanorods is 1.3 $\pm$ 0.2, while the nanorod in ionic liquid sample results in an α_{off} slope of 0.4 $\pm$ 0.1. Fits of the "on" probability distribution are not meaningful, due to the small number of "on" fluorescence events. The influence of the embedding medium on the blinking statistics reported here for nanorods is much larger than that observed previously for molecular dyes and nanoparticles embedded in organic polymers with similar dielectric constants.[52,53] The enhanced quenching observed here may be due to an increased number of trap states present on the surface of the nanorod, or it could be from the high electrical conductivity reported for the RTIL.[54] Detailed measurements with improved time resolution, using a series of ionic liquids at multiple excitation wavelengths, are necessary to determine the precise nature of the interaction between excited nanoparticles and RTILs. The results do show that a model invoking charge ejection to a distribution of surface or external trap states accounts for blinking when the excitation is well in excess of the band gap. The decrease in the power-law exponent for "off" events indicates an increased probability of observing long "off" periods. This result strongly supports the formation of a self-trapped exciton, after an energetic barrier has been overcome. The detailed excitation-wavelength study and the RTIL results suggest the barrier is in the region of 210−240 meV above the optical band gap. This type of model naturally provides for power-law distributions by assuming an exponentially large number of different traps over relatively short distances of a few nanometers. The efficiency of charge trapping in this case is strongly influenced by the environment.

The environment does not influence blinking statistics when excitation is near the band gap origin (Figure 8), indicating different blinking mechanisms may give rise to the two distinct categories of statistics observed. Power-law representations of nanoparticle fluorescence blinking have become quite ubiquitous, and recent studies on blinking of molecular dyes in both disordered and crystalline media result in similar probability distributions when recorded over long times.[52−64]

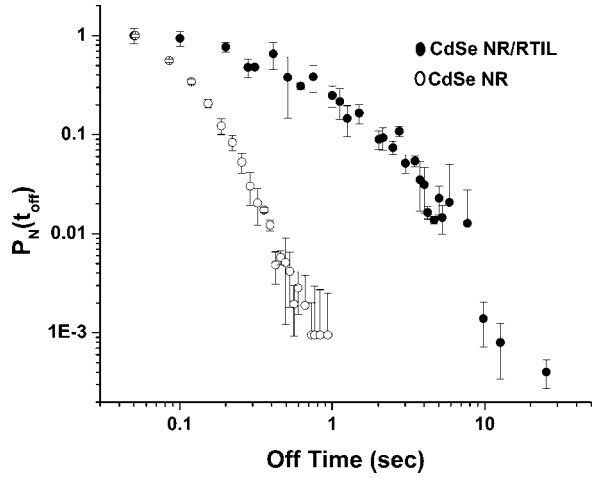

Figure 10. "Off"-time probability statistics for CdSe/TDPA nanorods when drop cast to a clean microscope coverslip (○), and when embedded in the RTIL (●). The "off" probability distribution shows a decreased negative slope when in the RTIL, indicative of more persistent "off" times. The slope fit to the "off" probability, using eq 2, provides a value of α_{off} = 0.4 (CdSe/NR RTIL) and α_{off} = 1.3 (CdSe/NR).

A number of models have been developed to account for these statistics. Of these, the two most prominent ones are based on a diffusion-controlled (trap-state energy) charge transfer mechanism[11,16−19,65] and another that attributes the power-law statistics to multiple charge trapping sites that have a vast range of recombination rates. The latter model can account for blinking statistics when the excitation energy is well in excess of the optical band gap. However, it is necessary to invoke a barrier at the interface that allows the charge carriers to access external traps as opposed to those on the interior of the nanoparticle.

It is possible that a trap-state energy, diffusion-controlled process gives rise to blinking when excitation is near the band gap resonance. The diffusion-controlled charge transfer mechanism accounts for power-law blinking statistics in CdSe nanocrystals by slow diffusion of the energies of trap states. In this model, a fluorescent nanoparticle blinks from "on" to "off" when the energy of a proximally close site of a dark state matches that of the bright state. The particle will remain in the "off" state until the energy of the trap again diffuses to match that of the bright state, satisfying the resonance condition for charge transfer. Diffusion of the trap-state energies is believed to be light-driven, similar to spectral diffusion of nanocrystal fluorescence.[21,22] Hence, the model predicts the critical time will depend on the excitation power density. In this work on nanorods and our previous work on nanocrystals,[15] a power dependence of the critical value is not observed for any excitation wavelength at room temperature. However, we note that the degree of spectral diffusion observed in CdSe nanocrystals also depends on the excitation wavelength.[41] This work does not preclude a diffusion-based model for nanoparticle blinking. In fact, diffusion-controlled charge transfer may be a critical early event for charge trapping. Nonetheless, the results clearly show the existence of an energetic barrier that changes the measured low-probability long-time blinking statistics of CdSe nanorods, providing strong evidence for surface or external trapping of charge carriers. Importantly, environmental influences only become significant when excitation is in excess of the optical band gap.

CONCLUSIONS

In conclusion, we have presented excitation-wavelength-dependent results for the fluorescence blinking statistics of single CdSe/TDPA nanorods over time intervals spanning milliseconds to minutes. The "on" statistics are found to be sensitive to the exciting wavelength, as are the "off" statistics. Qualitatively, the nanorods cycle from "on" to "off" configurations more frequently than nanocrystals with similar band gaps. The fluorescence blinking statistics of nanorods are analyzed for 10 different excitation wavelengths. The probability distribution for each wavelength is fit to a truncated power law. The truncation of the power law reflects a limitation to the duration of continuous "on" events. The fitting results can be grouped into two categories: (1) when excitation promotes the electron to an energy substantially above the band gap and (2) when the excitation frequency is near resonance with the first exciton transition. The data indicate a wavelength-dependent blinking mechanism that limits the continuous fluorescence emission efficiency of CdSe nanorods resulting from a distribution of nonemissive trap states. A possible explanation is that higher photon energies access external trap states more readily than when the minimum energy is used to create the charge carriers. To confirm this, the influences of an embedding RTIL matrix on the blinking statistics were measured as a function of the excess excitation energy. In particular, nanorods excited below the critical energetic threshold are not influenced by an embedding RTIL. However, when excitation energies exceed the threshold, blinking statistics are significantly dependent on the embedding matrix. The data suggest a threshold for charge carrier trapping in external and surface sites. This picture is consistent with a barrier to forming a self-trapped exciton. The findings suggest the performance efficiency of quantum-dot-based devices could be strongly dependent on the exciting wavelength. Further, from photon antibunching experiments, fluorescence emission across the entire length of the nanorod, as opposed to the existence of segmented domains, is confirmed, eliminating the possibility of the formation of multiple absorption and emission domains.

EXPERIMENTAL METHODS

The CdSe nanorods studied here are synthesized *via* a modified organometallic method in a coordinating solvent of trioctylphosphine oxide (TOPO) and TDPA based on the work of Peng *et al.*[26] The CdSe nanorods were produced in common air-free conditions on a nitrogen-filled Schlenk line. Briefly, 50 mg of CdO (Acros Organics #22379, 99%), 4.1 g of TOPO (Strem Chemicals #15-6661, 99%), and 305 mg of TDPA (PCI synthesis # 4671-75-4, 99%) were placed in a 50 mL three-neck flask with septa, thermometer, and refluxing column attached to the Schlenk line. In order to remove all residual water and oxygen from the mixture, the solution was heated to 120 °C under a nitrogen flow and subsequently vacuumed down for upward of 1 h. A 0.16 M SeTOP selenium−trioctylphosphine solution was prepared in a nitrogen-filled glovebox by placing 4 mL of technical grade trioctylphosphine (Aldrich #117854, 90%) and 42.0 mg of Se powder (Acros Organics #19807, 99% 200 mesh) into a scintillation vial and capped with a septum. After removal from the glovebox, the SeTOP solution was sonicated for 30−45 s to facilitate complete dissolution of the Se powder. After repeated nitrogen purge and vacuum cycles, the solution of CdO in TOPO/TDPA was optically clear with a slight golden tint occurring at

250 °C. Special care was taken that all CdO was completely dissolved and no residual CdO powder resided on the flask walls by vigorously shaking the vessel. At ~280 °C, a weak vacuum was applied to the CdO/TOPO/TDPA solution. A slight haze formed above the solution; the solution color changed to a darker golden hue, the vacuum was ceased, and a nitrogen flow was applied. With a solution temperature of 270 °C, 4.0 mL of the 0.16 M SeTOP was injected, and upon injection, the temperature decreased to 230 °C. Growth of the CdSe nanorods was performed at 260 °C, and the reaction was tracked *via* UV−vis spectrophotometry and photoluminescence (PL) spectrometry. Growth was allowed to continue for 5 min, then allowed to cool to approximately 50 °C, precipitated with methanol, and collected. Three precipitation and decantation cycles were performed, and the CdSe nanorods were ultimately dissolved in toluene. A representative TEM image of the resultant *ca.* 4 nm × 20 nm CdSe nanorods is found in Figure 1b.

The bulk room-temperature linear absorption and global photoluminescence (PL) spectra of the CdSe/TDPA nanorods are shown in Figure 1a. Linear absorption measurements are made on a dilute solution, and the PL measurements are obtained from a thin film of nanorods spin-coated to a silica substrate. The peak of the first exciton absorption transition is centered at 575 nm, and the absorption increases continuously to more energetic wavelengths. The PL spectrum is normalized to the ($1S_e-1S_h$; 575 nm) absorption transition for comparison. The peak of the PL is Stokes-shifted from the absorption by approximately 30 nm to a center value of 605 nm, and it has a full-width at half-maximum of 35 nm. From the bulk absorption and PL measurements, a CdSe diameter of approximately 4.0 nm can be inferred.

A dilute solution of the nanorods is dissolved in toluene and spin-coated onto a 0.17 mm thick microscope coverslip (refractive index (n_D) = 1.515) for single nanorod fluorescence measurements, resulting in a thin film of sparsely deposited particles. The coverslip is first cleaned by sonication in a Hellmanex II (Fluka) solution at 90 °C, followed by sonication in Millipore H_2O and followed by several rinse and sonication cycles to ensure removal of fluorescent impurities. The substrate is then passivated with *N*-(2-aminoethyl)-3aminopropyltrimethoxysilane (AEPS) prior to quantum dot deposition. The deposition of single particles is confirmed by atomic force microscopy and by photon antibunching measurements.

Single nanorod fluorescence trajectories are recorded using a home-built epifluorescence microscope. Two excitation sources are used: a continuous wave 543 nm laser and a high repetition rate wavelength-tunable femtosecond (fs) laser system. A Coherent Mira titanium sapphire oscillator produces ultrashort pulses that are amplified by a 200 kHz Coherent RegA regenerative amplifier, producing nominally 800 nm pulses with a temporal duration of 150 fs and pulse energies of 5 μJ. The laser output is split by a 70/30 beamsplitter to generate a 400 nm beam and a white-light continuum, which are then mixed in an optical parametric amplifier (Type I-BBO) to generate approximately 50 nJ of tunable output over a range of 500−700 nm. The intensities of both laser sources are attenuated with absorptive neutral density filters to provide average power densities at the sample ranging from 50 W/cm^2 to 10 kW/cm^2, spanning both linear and nonlinear multiphoton excitation regimes. The lowest power density employed corresponds to an average per rod exciton density of ≈0.15, taking into account the absorption strength. The excitation laser light is focused through the microscope slide onto the nanorod sample on the reverse side. A diffraction-limited spot is obtained by an oil immersion (n_D = 1.515) 1.3 NA objective (Nikon, PlanFluor 100), generating an approximately 200 nm spot size at the focus. An *x,y,z* translation stage is used to scan the sample through the excitation focal volume. Sample emission is collected through the same oil immersion objective and directed through a series of dichroic and notch filters to isolate the 605 nm band edge emission prior to imaging individual CdSe nanorods with a charge-coupled device (CCD) camera for detection. The signal is read out to a commercial video capture card and saved to a computer. The fluorescent point sources are temporally integrated to obtain fluorescence trajectories. The CCD detector has a minimum readout time of 10 ms, providing the limit to the temporal resolution. The signal-to-noise ratio achieved for single nanorod trajectories using 10 ms binning is ≈4. Averages and standard deviations reported throughout the text are reported to ±2σ.

Photon antibunching experiments were conducted with a commercial PicoQuant MicroTime200 time-resolved confocal microscope. The CdSe nanorods were excited with a single 400 nm photon generated by a variable repetition rate (1−20 MHz) laser (LDH, PicoQuant, 470 nm, 80 ps). Samples are spin-coated as described above and mounted on an Olympus IX71 platform. The excitation light is focused with a high numerical aperture objective (NA = 1.3), and the same objective is used to collect nanorod fluorescence. The emission is then split with a 50/50 beamsplitter and directed to two avalanche photodiode detectors (SPCM-AQR-14, Perkin-Elmer). Background fluorescence is rejected with band pass filters placed before the photodiodes. The photon pulses from the photodiodes are detected with time-correlated single-photon counting (TCSPC) electronics in combination with a four-channel router (PicoHarp 300; PicoQuant). The time resolution of 4 ps is achieved.

Absorption and fluorescence measurements of nanorods are also made in a high-dielectric environment. The CdSe/TDPA nanorods are spin-coated onto a clean coverslip that includes a silicone isolating well for fluids, purchased from Sigma. 1-Ethyl-3-methylimidizolium bis(trifluoromethylsulfonyl)imide ionic liquid is then added to the well, which is subsequently sealed by attaching a second coverslip that sandwiches the sample between the two microscope slides. The ionic liquid is used as purchased from Fluka, without further purification. The dielectric constant of this ionic liquid is 12.3.[51] Absorption measurements show no indication that the ionic liquid alters the exciton levels of the nanorods.

Acknowledgment. The authors gratefully acknowledge financial support by the Director, Office of Basic Energy Sciences, Chemical Sciences, Geosciences, and Biosciences Division, U.S. Department of Energy under Contract No. DE-AC02-05CH11231. J.Z.Z. acknowledges financial support from the BES division of the Department of Energy, Grant No. 05ER4623A00. The authors also thank Thomas Huser and Samantha Fore, University of California, Davis, for assistance with photon antibunching measurements.

REFERENCES AND NOTES

1. Murray, C. B.; Norris, D. J.; Bawendi, M. G. Synthesis and Characterization of Nearly Monodisperse CdE (E = S, Se, Te) Semicondutor Nanocrystallites. *J. Am. Chem. Soc.* **1993**, *115*, 8706–8715.
2. Klimov, V. I.; Mikhailovsky, A. A.; Xu, S.; Mlko, A.; Hollingsworth, J. A. Optical Gain and Stimulated Emission in Nanocrytsal Quantum Dots. *Science* **2000**, *290*, 314–317.
3. Huynh, W. U.; Dittmer, J. J.; Alivisatos, A. P. Hybrid Nanorod-Polymer Solar Cells. *Science* **2002**, *290*, 2425–2427.
4. Bruchez, M. P.; Moronne, M.; Gin, P.; Weiss, S.; Alivisatos, A. P. Semiconductor Nanocrystals as Fluorescent Biological Labels. *Science* **1998**, *281*, 2013–2016.
5. Peng, X.; Manna, L.; Yang, W.; Wickham, J; Scher, E.; Kadavanich, A.; Alivisatos, A. P. Shape Control of CdSe Nanocrystals. *Nature* **2000**, *404*, 59–61.
6. Huynh, W. U.; Peng, X.; Alivisatos, A. P. CdSe Nanocrystal Rods/Poly(3-hexylthiophene) Composite Photovoltaic Devices. *Adv. Mater.* **1999**, *11*, 923–927.
7. Nirmal, M.; Dabbousi, B. O.; Bawendi, M. G.; Macklin, J. J.; Trautman, J. K.; Harris, T. D.; Brus, L. E. Fluorescence Intermittency in Single Cadmium Selenide Nanocrystals. *Nature* **1996**, *383*, 802–804.
8. Kuno, M.; Fromm, D. P.; Hamann, H. F.; Gallagher, A.; Nesbitt, D. J. Nonexponential "Blinking" Kinetics of Single CdSe Quantum Dots: A Universal Power Law Behavior. *J. Chem. Phys.* **2000**, *112*, 3117–3120.
9. Kuno, M.; Fromm, D. P.; Hamann, H. F.; Gallagher, A.; Nesbitt, D. J. "On/Off" Fluorescence Intermittency of Single Semiconductor Quantum Dots. *J. Chem. Phys.* **2001**, *115*, 1028–1040.

10. Kuno, M.; Fromm, D. P.; Johnson, S. T.; Gallagher, A.; Nesbitt, D. J. Modeling Distributed Kinetics in Isolated Semiconductor Quantum Dots. *Phys. Rev. B* **2003**, *67*, 125304.
11. Shimizu, K. T.; Neuhauser, R. G.; Leatherdale, C. A.; Empedocles, S. A.; Woo, W. K.; Bawendi, M. G. Blinking Statistics in Single Semiconductor Nanocrystal Quantum Dots. *Phys. Rev. B* **2001**, *63*, 205316.
12. Kuno, M.; Fromm, D. P.; Hamann, H. F.; Gallagher, A.; Nesbitt, D. J. Fluorescence Intermittency in Single InP Quantum Dots. *Nano Lett.* **2001**, *1*, 557–564.
13. Glennon, J. J.; Tang, R.; Buhro, W. E.; Loomis, R. A. Synchronous Photoluminescence Intermittency (Blinking) along Whole Semiconductor Quantum Wires. *Nano Lett.* **2007**, *7*, 3290–3295.
14. Wang, S.; Querner, C.; Emmons, T.; Drndic, M.; Crouch, C. H. Fluorescence Blinking Statistics from Core and Core/Shell Nanorods. *J. Phys. Chem. B* **2006**, *110*, 23221–23227.
15. Knappenberger, K. L., Jr.; Wong, D. B.; Romanyuk, Y. E.; Leone, S. R. Excitation Wavelength Dependence of Fluorescence Intermittency in CdSe/ZnS Core/Shell Quantum Dots. *Nano Lett.* **2007**, *7*, 3869–3874.
16. Tang, J.; Marcus, R. A. Mechanisms of Fluorescence Blinking in Semiconductor Nanocrystal Quantum Dots. *J. Chem. Phys.* **2005**, *123*, 054704.
17. Tang, J.; Marcus, R. A. Diffusion-Controlled Electron Transfer Processes and Power-Law Statistics of Fluorescence Intermittency of Nanoparticles. *Phys. Rev. Lett.* **2005**, *95*, 107401.
18. Tang, J.; Marcus, R. A. Single Particle *versus* Ensemble Average: From Power-Law Intermittency of a Single Quantum Dot to a Quasistretched Exponential Fluorescence Decay of an Ensemble. *J. Chem. Phys.* **2005**, *123*, 204511.
19. Frantsuzov, P. A.; Marcus, R. A. Explanation of Quantum Dot Blinking without the Long-Lived Trap Hypothesis. *Phys. Rev. B* **2005**, *72*, 155321.
20. Verberk, R.; van Oijen, A. M.; Orrit, M. Simple Model for the Power-Law Blinking of Single Semiconductor Nanocrystals. *Phys. Rev. B* **2002**, *66*, 233202.
21. Empedocles, S. A.; Bawendi, M. G. Influence of Spectral Diffusion on the Line Shapes of Single CdSe Nanocrystallite Quantum Dots. *J. Phys. Chem. B* **1999**, *103*, 1826–1830.
22. Neuhauser, R. G.; Shimizu, K. T.; Woo, W. K.; Empedocles, S. A.; Bawendi, M. G. Correlation between Fluorescence Intermittency and Spectral Diffusion in Single Semiconductor Quantum Dots. *Phys. Rev. Lett.* **2000**, *85*, 3301–3304.
23. Krauss, T. D.; Brus, L. E. Charge, Polarizability, and Photoionization of Single Semiconductor Nanocrystals. *Phys. Rev. Lett.* **1999**, *83*, 4840–4843.
24. Glennon, J. J.; Buhro, W. E.; Loomis, R. A. Simple Surface-Filling-Trap Model for Photoluminscence Blinking in Spanning Entire CdSe Quantum Wires. *J. Phys. Chem. C* **2008**, *112*, 4813–4817.
25. Protasenko, V. V.; Hull, K. L.; Kuno, M. Disorder-Induced Optical Heterogeneity in Single CdSe Nanowires. *Adv. Mater.* **2005**, *17*, 2942–2949.
26. Peng, Z. A.; Peng, X. Nearly Monodisperse and Shape-Controlled CdSe Nanocrystals *via* Alternative Routes: Nucleation and Growth. *J. Am. Chem. Soc.* **2002**, *124*, 3343–3353.
27. Stoler, D. Photon Antibunching and Possible Ways to Observe It. *Phys. Rev. Lett.* **1974**, *33*, 1397–1400.
28. Kimble, H. J.; Dagenais, M.; Mandel, M. Photon Anti-Bunching in Resonance Fluorescence. *Phys. Rev. Lett.* **1977**, *39*, 691–694.
29. Laurence, T. A.; Fore, S.; Huser, T. Fast, Flexible Algorithm for Counting Fluorescence Correlations. *Opt. Lett.* **2006**, *31*, 829–831.
30. Fore, S.; Laurence, T. A.; Hollars, C. W.; Huser, T. Counting Constituents in Molecular Complexes by Photon Antibunching. *IEEE J. Quantum Electron.* **2007**, *13*, 996–1005.
31. Michler, P.; Imamoglu, A.; Mason, M. D.; Carson, P. J.; Strouse, G. F.; Buratto, S. K. Quantum Correlation among Photons from a Single Quantum Dot at Room Temperature. *Nature* **2000**, *406*, 968–970.
32. Borgstrom, M. T.; Zwiller, V.; Muller, E.; Imamoglu, A. Optically Bright Quantum Dots in Single Nanowires. *Nano Lett.* **2005**, *5*, 1439–1443.
33. Michler, P.; Imamoglu, A.; Kiraz, A.; Becher, C.; Mason, M. D.; Carson, P. J.; Strouse, G. F.; Buratto, S. K.; Schoenfeld, W. V.; Petroff, P. M. Nonclassical Radiation from a Single Quantum Dot. *Phys. Status Solidi* **2002**, *229*, 399–405.
34. Kumar, P.; Mehta, A.; Dadmun, M. D.; Zheng, J.; Peyser, L.; Bartko, A. P.; Dickson, R. M.; Thundat, T.; Sumpter, B. G.; Noid, D. W.; et al. Narrow-Bandwidth Spontaneous Luminescence from Oriented Semiconducting Polymer Structures. *J. Phys. Chem. B* **2003**, *107*, 6252–6257.
35. Messin, G.; Hermier, J. P.; Giacobino, P.; Desbiolles; Dahan, M. Bunching and Antibunching in the Fluorescence of Semiconductor Nanocrystals. *Opt. Lett.* **2001**, *26*, 1891–1893.
36. Kagan, C. R.; Murray, C. B.; Bawendi, M. G. Long-Range Resonance Transfer of Electronic Excitations in Close-Packed CdSe Quantum Dot Solids. *Phys. Rev. B* **1996**, *54*, 8633–8643.
37. Fomenko, V.; Nesbitt, D. J. Solution Control of Radiative and Nonradiative Lifetimes: A Novel Contribution to Quantum Dot Blinking Supression. *Nano Lett.* **2008**, *8*, 287–293.
38. Zhang, K.; Chang, H.; Fu, A.; Alivisatos, A. P.; Yang, H. Continuous Distribution of Emissive States from Single CdSe/ZnS Quantum Dots. *Nano Lett.* **2006**, *6*, 843–847.
39. Heyes, C. D.; Kobitski, A. Y.; Breus, V. V.; Nienhaus, G. U. Effect of the Shell on the Blinking Statistics of Core−Shell Quantum Dots: A Single Particle Fluorescence Study. *Phys. Rev. B* **2007**, *75*, 125431.
40. Dabbousi, B. O.; Rodriguez-Viejo, J.; Mikulek, F. V.; Heine, J. R.; Mattoussi, H.; Ober, R.; Jensen, K. F.; Bawendi, M. G. (CdSe)ZnS Core−Shell Quantum Dots: Synthesis and Characterization of a Size Series of Highly Luminescent Nanocrystallites. *J. Phys. Chem. B* **1997**, *101*, 9463–9475.
41. Berrettini, M. G.; Braun, G.; Hu, J. G.; Strouse, G. F. NMR Analysis of Surfaces and Interfaces in 2 nm CdSe Nanocrystals. *J. Am. Chem. Soc.* **2004**, *126*, 7063–7070.
42. Tachiya, M.; Mozumder, A. Model of Pre-existing Traps for Electrons in Polar Glasses. *J. Chem. Phys.* **1974**, *60*, 3037–3041.
43. Hoheisel, W.; Colvin, V. L.; Johnson, C. S.; Alivisatos, A. P. Threshold for Quasi-Continuum Absorption and Reduced Luminescence Efficiency in CdSe Nanocrystals. *J. Chem. Phys.* **1994**, *101*, 8455–8460.
44. Rumbles, G.; Selmarten, D. C.; Ellingson, R. J.; Blackburn, J. L.; Yu, P.; Smith, B. B.; Micic, O. I.; Nozik, A. J. Anomalies in the Linear Absorption, Transient Absorption, Photoluminscence and Photoluminscence Excitation Spectroscopies of Colloidal InP Quantum Dots. *J. Photochem. Photobiol. A: Chem.* **2001**, *142*, 187–195.
45. Ellingson, R. J.; Blackburn, J. L.; Yu, P.; Rumbles, G.; Micic, O. I.; Nozik, A. J. Excitation Energy Dependent Efficiency of Charge Carrier Relaxation and Photoluminescence in Colloidal InP Quantum Dots. *J. Phys. Chem. B* **2002**, *106*, 7758–7765.
46. Schill, A. W.; Gaddis, C. S.; Qian, W.; El-Sayed, M. A.; Cai, Y.; Milan, V. T.; Sandhage, K. Ultrafast Electronic Relaxation and Charge-Carrier Localization in CdSe/CdSe/CdS Quatnum Dot−Quantum Well Heterostructures. *Nano Lett.* **2006**, *6*, 1940–1949.
47. Rosen, A. L.; Efros, M. The Electronic Structure of Semiconductor Nanocrystals. *Annu. Rev. Mater. Sci.* **2000**, *30*, 475–521.
48. Wang, C.; Shim, M.; Guyot-Sionnest, P. Electrochromic Nanocrystal Quantum Dots. *Science* **2001**, *291*, 2390–2392.
49. Pandey, A.; Guyot-Sionnest, P. Multicarrier Recombination in Colloidal Quantum Dots. *J. Chem. Phys.* **2007**, *127*, 111104.

50. Israelachvili, J. *Intermolecular and Surface Forces*, 2nd ed.; Academic Press: San Diego, 1992.
51. Weingartner, H. The Static Dielectric Constant of Ionic Liquids. *Z. Phys. Chem.* **2006**, *220*, 1395–1405.
52. Schuster, J.; Cichos, F.; von Borczyskowski, C. Influence of Self-Trapped States in the Fluorescence Intermittency of Single-Molecules. *Appl. Phys. Lett.* **2005**, *87*, 051915.
53. Issac, A.; von Borczyskowski, C.; Cichos, F. Correlation Between Photoluminescence Intermittency of CdSe Quantum Dots and Self-Trapped States in Dielectric Media. *Phys. Rev. B* **2005**, *71*, 161302.
54. Schroder, C.; Haberler, M.; Steinhauser, O. On the Computation and Contribution of Conductivity in Molecular Ionic Liquids. *J. Chem. Phys.* **2008**, *128*, 134501.
55. Zondervan, R.; Kulzer, F.; Orlinskii, S. B.; Orrit, M. Photoblinking of Rhodamine 6G in Poly(vinyl alcohol) at the Ensemble and Single-Molecule Levels. *J. Phys. Chem. A* **2003**, *107*, 6770–6776.
56. Haase, M.; Hubner, C. G.; Reuther, E.; Hermann, A.; Mullen, K.; Basche, T. Exponential and Power-Law Kinetics of Single-Molecule Fluorescence Intermittency. *J. Phys. Chem. B* **2004**, *108*, 10445–10450.
57. Schuster, J.; Cichos, F.; von Borczyskowski, C. Blinking of Single Molecules in Various Environments. *Opt. Spectrosc.* **2005**, *98*, 712–717.
58. Yeow, E. K. L.; Melnikov, S. M.; Bell, T. D. M.; De Schryver, F. C.; Hofkens, J. Characterizing the Fluorescence Intermittency and Photobleaching Kinetics of Kinetics of Dye Molecules Immobilized on a Glass Surface. *J. Phys. Chem. A* **2006**, *110*, 1726–1734.
59. Cichos, F.; von Borczyskowski, C.; Orrit, M. Power-Law Intermittency of Single Emitters. *Curr. Opin. Colloid. Interface Sci.* **2007**, *12*, 272–284.
60. von Borczyskowski, C.; Cichos, F.; Martin, J.; Schuster, J.; Issac, A.; Brabandt, J. Common Luminescence Intensity Fluctuations of Single Particles and Single Molecules in Non-Conducing Matrices. *Eur. Phys. J. Special Topics* **2007**, *144*, 13–25.
61. Wustholz, W. J.; Bott, E. D.; Isborn, C. M.; Li, X.; Kahr, B.; Reid, P. J. Dispersive Kinetics From Single Molecules Oriented in Single Crystals of Potassium Acid Phthalate. *J. Phys. Chem. C* **2007**, *111*, 9146–9156.
62. Clifford, J. N.; Bell, T. D. M.; Tinnefeld, P.; Heilemann, M.; Melnikov, S. M.; Hotta, J.; Sliwa, M.; Dedecker, P.; Sauer, M.; Hofkens, J.; et al. Fluorescence of Single Molecules in Polymer Films: Sensitivity of Blinking to Local Environment. *J. Phys. Chem. B* **2007**, *111*, 6987–6991.
63. Wustholz, K. L.; Sluss, D. R. B.; Kahr, B.; Reid, P. J. Applications of Single-Molecule Microscopy to Problems in Dyed Composite Materials. *Int. Rev. Phys. Chem.* **2008**, *27*, 167–200.
64. Wustholz, K. L.; Bott, E. D.; Kahr, B.; Reid, P. J. Memory and Spectral Diffusion in Single-Molecule Emission. *J. Phys. Chem. C* **2008**, *112*, 7877–7885.
65. Pelton, M.; Smith, G.; Scherer, N. F.; Marcus, R. A. Evidence for a Diffusion-Controlled Mechanism for Fluorescence Blinking in Colloidal Quantum Dots. *Proc. Natl. Acad. Sci. U.S.A.* **2007**, *104*, 14249–14254.